Feedback Network Controls Photoreceptor Output at the of First Layer of Visual Synapses in *Drosophila*

Lei Zheng, Gonzalo G. de Polavieja, Verena Wolfram, Musa H. Asyali, Roger C. Hardie, and Mikko Juusola

Neither Lateral Synaptic Connections in Lamina nor ERG Are the Cause for the Peak in Noise Variance of Photoreceptors

We recorded voltage output of WT photoreceptors and extracellular field potentials or electroretinograms (ERGs) in response to naturalistic light stimuli from small circular fields of different sizes. These experiments allowed us to test weather the used 5° stimulus was small enough to prevent lateral connectivity in the eye influencing the voltage response of individual photoreceptors. Fig. 1 A shows no significant differences between the responses to 1° and 5° stimuli.Also the ERGs were relatively small even during the bright NS (Fig. 1 A). The power spectra of ERGs did not contain

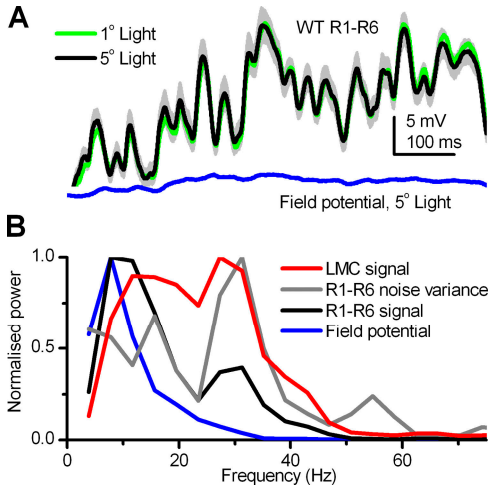

Figure 1. Comparison between different electrical responses and power spectra. (A) Average voltage responses of a WT photoreceptor to 1° (green) and 5° (black) NS presented at the center of the receptive field. ERG (blue) measured extracellularly after photoreceptor recordings. Responses (n = 20) to 1° and 5° light stimuli have no significant differences (mean ± SD; gray). The field potential amplitude is too small to have a significant influence on the photoreceptor response. (B) Normalized power spectra ERG (blue), average response of LMCs (red) and photoreceptors (black) and photoreceptor noise variance (gray). Data is for WT. The relevant frequencies of the noise variance correlate only with the LMC signal. The ERG signal contains only very low frequencies and cannot be responsible for the photoreceptor noise variance.

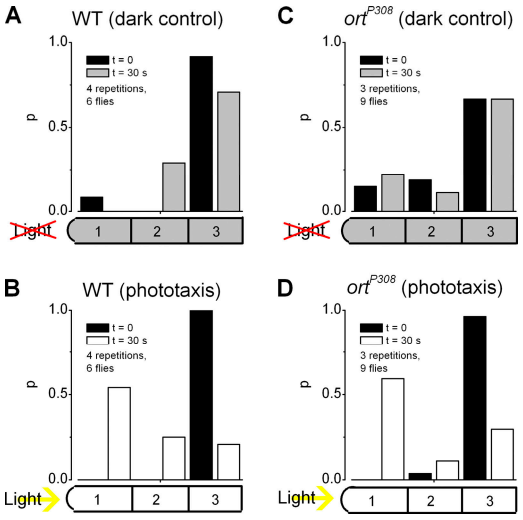

Figure 2. (A) WT control. Probability of finding the fly in each region of the tube at t = 0 (black bars) and at t = 30 s (gray bars) with the cold light off during the experiment. Statistics were gathered repeating the experiment 4 times for 6 different flies. For the majority of cases, we find the flies initially in Region 3 and after the 30 s still in Region 3. This control shows that there are no significant after-effects of antigravitaxis or nonvisual cues making the flies to go to Region 1. (B) WT phototaxis. Probability of finding the fly in each region of the tube at t = 0 (black bars) and at t = 30 (white bars). The cold lamp is switched on at t = 0. While initially we find all flies in Region 3, after 30 s in 54% of the cases, the flies are in Region 1 and only 21% remain in Region 3. Typically, the flies run from Region 3 to Region 1 in an almost straight line. 2 in 6 flies did not respond to the test and flies that responded to the test showed very little variability in different repetitions. (C) ort^{P306} control. Analogous to A but for the ort^{P306} flies. Statistics were gathered repeating the experiment 3 times for 9 different flies. Similarly to the WT flies, ort^{P306} flies remained at Region 3, although they were slightly more reticent to go to Region 3 by antigravitaxis. (D) ort^{P306} phototaxis. Analogous to B but for ort^{P306} flies. Results are very similar to WT: 59% of the cases are in Region 3 at t = 30 s and 30% remain in Region 3. ort^{P306} flies initially in Region 3 tend to migrate to Region 1 when the cold light is on. 2 out of 9 flies did not respond to the test, but most flies that did respond ran directly to Region 1.

J. Gen. Physiol. © The Rockefeller University Press
Cite by DOI:10.1085/jgp.200509470
http://www.jgp.org/cgi/doi/10.1085/jgp.200509470

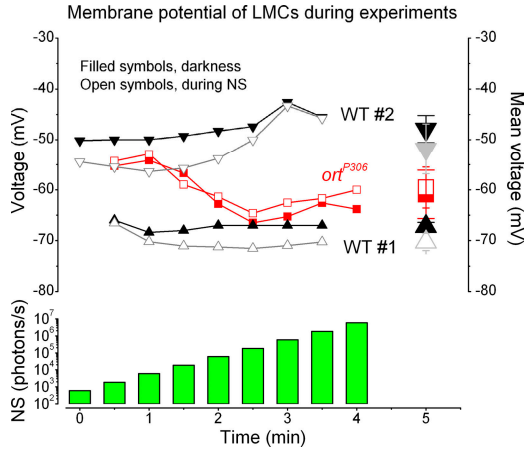

Figure 3. Mean membrane potential of WT and *ort*^{P306} LMCs varied between −40 and −70 mV, but remained relatively constant during individual experiments. WT #1 and WT #2 are recording series from the same LMC, 20 min apart. In both cases the mean membrane potential, before and during naturalistic light stimulation (NS), changed <5 mV over the experiments. Since the mean LMC voltage remained practically unchanged when the stimulation was repeatedly altered from darkness to naturalistic stimulation (NS) of different luminance, the mean light intensity had only a small influence on the mean LMC output. Yet, for the second experiment, the LMC had depolarized 20 mV from the previous values. This behavior did not reduce the size (or variance) of LMC responses to NS (not depicted). In general, slow drifts in the mean membrane potential are typical for long-lasting LMC recordings and may indicate gradual changes in the physiological state of the animal, the laminal network, or both (Hardie, 1988; Juusola et al., 1995). *ort*^{P306} had a mean membrane potential around −60 mV for both darkness and NS. These low values are in line with our feedback model, as they indicate that when in rest, the tonic feedback component from *ort*^{P306} LMCs to photoreceptor terminals should not differ from that of WT LMCs. Accordingly, the dark resting potentials and membrane impedances of *ort*^{P306} and WT photoreceptors did not show significant differences (Fig. 4, C and D, respectively).

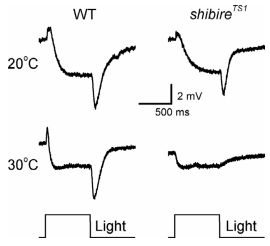

Figure 4. Typical ERG responses. On- and off-transients, attributed to synaptic transmission across the first visual synapse, disappear from the ERG of *shibire*^{TS1} when these mutants are warmed to ≥28°C. In contrast, the transients in WT ERG show little temperature sensitivity. The data is in line with the findings of Chen and Stark (1990).

high frequencies that are present in the noise variance of photoreceptors and in the LMC signals (Fig. 1 B). Since these components were also relatively weakly represented by photoreceptor signals, this suggests that much of the high frequency noise in photoreceptors come from synaptic feedbacks from the primary visual interneurones.

ort^{P306} and WT Flies Show the Same Phototactic Behavior

We performed a simple phototactic test using WT and *ort*^{P306} flies to show that the malfunctioning first visual synapse does not make *ort*^{P306} mutants blind. A glass tube of 10 cm length and 3 cm diameter was used as behavioral arena. Small marks on the outside of the tube indicated three regions of equal size. The tube opening is in Region 3 and was closed with compressed cotton, covered with black plastic to avoid reflection of light. After taking a single fly in the tube, the tube was closed and placed in dim light in a vertical position (Region 3 up) for 30 s so the fly typically runs against gravity to Region 3. In this way, we have the fly initially away from Region 1 and active. The tube is then placed horizontally at time $t = 0$ in a box in darkness. A fiber optic connected to a cold lamp enters the box through a small hole and is placed 1 cm away from Region 1 of the tube. We either keep the cold lamp off (dark control) or we switch it on at $t = 0$ (phototaxis test). At $t = 30$ s, we check in which region of the tube the fly is (Fig. 2). These results show that WT and *ort*^{P306} flies show the same phototactic behavior. The experiments were done at room temperature (~22°C).

Mean Membrane Potential of LMCs during Long Experiments In Vivo

High quality microelectrode penetrations allowed LMC recordings that could last for many minutes. Fig. 3 illustrates changes in the mean membrane potential of WT and *ort*^{P306} LMCs during continuous experiments at different luminances.

ERGs of *shibire*^{TS1} and WT Flies

We tested the temperature sensitivity of synaptic transmission in *shibire*^{TS1} mutants by examining the on- and off-transients of the ERGs at different temperatures. Fig. 4 compares typical ERG recordings from WT flies and *shibire*^{TS1} mutants at 20°C and 30°C.

Voltage Responses of *shibire*^{TS1} and WT Flies

We tested the effect of synaptic feedbacks on the voltage responses of photoreceptors by comparing the responses of *shibire*^{TS1} and WT photoreceptors at 20°C and 30°C. These data are shown in Fig. 5.

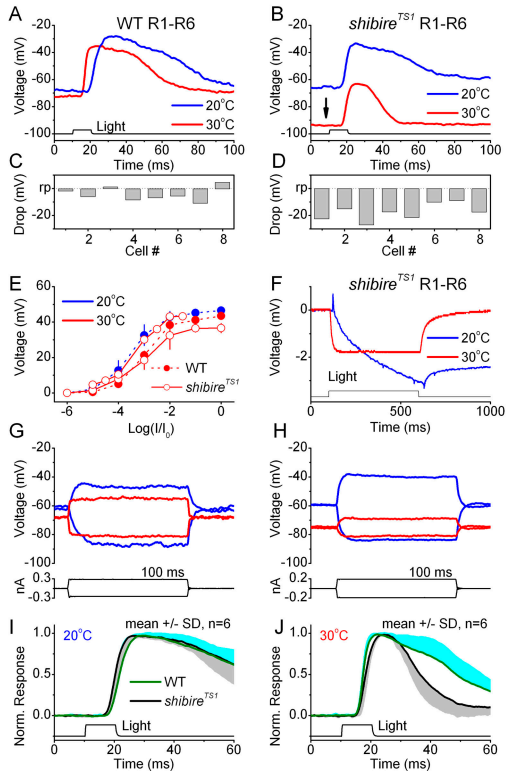

Figure 5. Intracellular photoreceptor data. A and B show voltage responses of dark-adapted WT and *shibire*^{TS1} photoreceptors to a saturating light pulse, respectively. The intracellular recordings were done first at 20°C (blue traces) and repeated after warming at 30°C (red traces) from the same cells. The light stimulus was always delivered at the center of the receptive field. Warming accelerated the rise of the responses and shortened their duration. However, the rise was more affected in WT cells, whereas the responses of *shibire*^{TS1} photoreceptors were briefer. Warming also hyperpolarized the dark resting potential of the cells, WT: -3.0 ± 5.2 mV ($n = 8$) and *shibire*^{TS1}: $-17.5 \pm .\ 6.2$ mV ($n = 8$). This drop in potential is shown for the corresponding eight photoreceptors: WT (C) and *shibire*^{TS1} (D). E shows the typical sizes of the voltage responses of WT and *shibire*^{TS1} photoreceptors to 10-ms light pulses of different intensity at 20°C and 30°C. The sensitivity of the cells was similar, indicating that the phototransduction reactions of *shibire*^{TS1} were not compromised by warming (WT cool, $n = 3$; WT warm, $n = 1$; *shibire*^{TS1} warm, $n = 3$; *shibire*^{TS1} cool, $n = 1$). (F) The ERGs of a *shibire*^{TS1} fly to a saturating light pulse, measured after the intracellular experiments. At 30°C, ERG shows no transients, but after cooling for 10 min both on- and off-transients reappear. The data is from the same fly as in B. G and H show voltage responses of a WT photoreceptor and a *shibire*^{TS1} photoreceptor, respectively, to small hyperpolarizing and depolarizing current pulses, injected intracellularly. The peak membrane impedances (V/I) of the cells were typically >100 MΩ at 20°C (blue traces), but in both cases warming to 30°C more than halved them (see Juusola and Hardie, 2001). Membrane impedance influences the speed of the voltage responses: the lower the impedance the faster the membrane charges the voltage responses. The relative similarity of the impedances enables us to approximate the effect of synaptic feedback as the difference between the corresponding voltage responses of WT and *shibire*^{TS1} photoreceptors. I and J respectively. SDs of the responses are shown as light blue (WT) and gray (*shibire*^{TS1}) shading. At 20°C, the responses of WT and *shibire*^{TS1} photoreceptors did not differ significantly, although the rising phase of the responses in *shibire*^{TS1} cells appeared slightly faster. At 30°C, the rising phase of the responses was faster in WT photoreceptors and their responses also outlasted the responses of *shibire*^{TS1} photoreceptors. Both cells showed variability in the speed on the responses, as indicated by the delayed broadening of their SDs. Some of this variability must come from the variable impedances of the cells, influenced by the recording location and the quality of the cell impalements. However, regardless of the mean size and speed of the responses, the findings appear ever clearer when one compares the recordings from the same cells at cool and warm temperatures; the warming accelerated the rising phase of the responses of the WT photoreceptors significantly more than those of the *shibire*^{TS1} photoreceptors to the same light stimulus. Hence, our data strongly suggests that the feedback conductances at axon terminals participate in shaping the voltage responses of *Drosophila* photoreceptors.

Light Current Statistics

TABLE I

Statistics of Phototransduction Parameters in WT and ort^{P306}

	Impulse time-to-peak (ms)	Impulse amplitude (pA)	Bump amplitude (pA)	Bump life time (ms)	Quantum efficiency rate
WT	43.9 ± 3.0 (n = 8)	390 ± 88 (n = 9)	9.7 ± 1.2 (n = 29)	19.5 ± 3.2 (n = 29)	2.4 ± 0.3 (n = 8)
ort^{P306}	44.4 ± 0.7 (n = 10)	424 ± 106 (n = 10)	10.9 ± 2.0 (n = 10)	17.3 ± 3.3 (n = 10)	2.5 ± 0.7 (n = 10)

Whole-cell recordings of dissociated photoreceptors. Recordings of bumps consisted of 17–72 responses to single photons (mean ± SD).

Parameters for Entropy Calculations

TABLE II

Extrapolation Parameters Used for Calculating the Rate of Information Transfer

	Total entropy	Noise entropy
$size \to \infty$	$H_S^{T,\nu,size} = H_S^{T,\nu} + H_{S,1}^{T,\nu}/size + H_{S,2}^{T,\nu}/size^2$ size being 3/10, 4/10,…10/10 of data	$H_N^{T,\nu,size} = H_N^{T,\nu} + H_{N,1}^{T,\nu}/size + H_{N,2}^{T,\nu}/size^2$ *size* being 3/10, 4/10,…10/10 of data
$v \to \infty$	$H_S^{T,\nu} = H_S^T + H_{S,1}^T/\nu$ ν = 6–13	$H_N^{T,\nu} = H_N^T + H_{N,1}^T/\nu$ ν = 6–13
$T \to \infty$	$R_S^T = R_S + R_{S,1}T^{-1}$ calculated using 3–6 linearly aligned points.	$R_N^T = R_N + R_{N,1}T^{-1}$ calculated using 2–5 linearly aligned points.

REFERENCES

Chen, D.-M., and W.S. Stark. 1990. The effects of temperature on visual receptors in temperature-sensitive paralytic paralytic *shibire* (shits) mutant *Drosophila*. *J. Insect Physiol.* 39:385–392.

Hardie, R.C. 1988. Effects of antagonists on putative histamine receptors in the first visual neuropile of the housefly (*Musca domestica*). *J. Exp. Biol.* 138:221–241.

Juusola, M., R.O. Uusitalo, and M. Weckström. 1995. Transfer of graded potentials at the photoreceptor-interneuron synapse. *J. Gen. Physiol.* 105:117–148.

Juusola, M., and R.C. Hardie. 2001. Light adaptation in *Drosophila* photoreceptors: II. Rising temperature increases the bandwidth of reliable signaling. *J. Gen. Physiol.* 117:27–42.